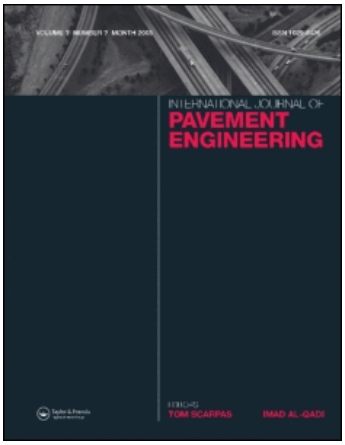

International Journal of Pavement Engineering
Publication details, including instructions for authors and subscription information:
http://www.informaworld.com/smpp/title~content=t713646742

An evaluation of the built-in temperature difference input parameter in the jointed plain concrete pavement cracking model of the Mechanistic-Empirical Pavement Design Guide

J. M. Vandenbossche[a]; F. Mu[a]; J. J. Gutierrez[a]; James Sherwood[b]
[a] Department of Civil and Environmental Engineering, University of Pittsburgh, Pittsburgh, PA, USA [b] Federal Highway Administration, McLean, VA, USA

First published on: 01 June 2010

To cite this Article Vandenbossche, J. M. , Mu, F. , Gutierrez, J. J. and Sherwood, James(2010) 'An evaluation of the built-in temperature difference input parameter in the jointed plain concrete pavement cracking model of the Mechanistic-Empirical Pavement Design Guide', International Journal of Pavement Engineering,, First published on: 01 June 2010 (iFirst)
To link to this Article: DOI: 10.1080/10298436.2010.489113
URL: http://dx.doi.org/10.1080/10298436.2010.489113

International Journal of Pavement Engineering
iFirst article, 2010, 1–14

Taylor & Francis
Taylor & Francis Group

An evaluation of the built-in temperature difference input parameter in the jointed plain concrete pavement cracking model of the Mechanistic–Empirical Pavement Design Guide

J.M. Vandenbossche[a]*, F. Mu[a1], J.J. Gutierrez[a2] and James Sherwood[b3]

[a]*Department of Civil and Environmental Engineering, University of Pittsburgh, Pittsburgh, PA, USA;* [b]*Federal Highway Administration, McLean, VA, USA*

(*Received 15 July 2009; final version received 23 April 2010*)

This paper evaluates the implementation of the built-in temperature difference input parameter in the Mechanistic–Empirical Pavement Design Guide (MEPDG) for the design of jointed plain concrete pavements (JPCPs). The pavement distress, in terms of transverse cracking, is expected to be minimised when the transient temperature difference is equal in magnitude to the built-in temperature difference but of the opposite sign. However, this study shows that a built-in temperature difference of −6.5°C minimises the cracking prediction for JPCPs. This optimum value of −6.5°C coincides with the default value in the MEPDG of −5.5°C, which was established through the nationwide calibration. The cause of this phenomenon is further investigated by taking into account the traffic loading time, slab thickness, joint spacing and reversible shrinkage, but none of these factors are able to explain this anomaly. The results from this study indicate that the built-in gradient should not be an input but is merely a calibration constant. A comparison between predictions using the measured and default built-in temperature difference again supports that it is better characterised as a calibration constant.

Keywords: MEPDG; built-in temperature difference; jointed plain concrete pavement; cracking; traffic distribution

1. Impetus

The treatment of the permanent built-in temperature difference input parameter in the Mechanistic–Empirical Pavement Design Guide (MEPDG; ARA, Inc., ERES Division 2004) deserves study because the MEPDG performance prediction models were calibrated using a constant value for this input while it is left as a modifiable input parameter for users. This study attempts to better understand the effects of the input value for built-in temperature difference on predicted jointed plain concrete pavement (JPCP) cracking and to characterise the factors that influence this relationship. An evaluation is performed to determine whether changes in the input value of this variable produce reasonable changes in MEPDG-predicted transverse cracking. A comparison using the MEPDG default value against the actual measurement is made to reveal whether the input value should be set as a constant.

2. Background

The MEPDG developed under the National Cooperative Highway Research Program Project 1-40 is an analysis and design tool that considers factors representing all of the design inputs considered in the American Association of State Highway Transportation Officials 1993 pavement design procedure. It also attempts to account, in a very comprehensive manner, for some of the key mechanisms that are known to affect pavement performance. The outputs of the new procedure include the predicted quantities of distress (i.e. cracking, spalling and faulting) and ride quality (i.e. international roughness index) for JPCPs present at any given time.

One of the most important improvements in the new procedure is the direct consideration of climatic effects (e.g. the development of temperature and moisture gradients in concrete paving slabs and their effect on pavement stresses and deformations), which are modelled using the Enhanced Integrated Climatic Model (EICM), incorporated in the MPEDG. The EICM is capable of predicting temperature and moisture conditions through the depth of the pavement structure (i.e. it is a one-dimensional model) on an hourly basis.

The mechanistic response of the pavement structure to the interaction between traffic (which is considered using actual axle load spectra as opposed to equivalent single axle loads) and environmental loads in the context of the material and structural properties of the pavement is managed by a neural network (NN) that is based on finite-element method analyses and incorporated in the MEPDG. By coupling the NN and the EICM, the MEPDG is able to analyse the performance of pavements on an incremental basis so that the damage caused by each load can be determined in consideration of the temperature and moisture gradients present in the slab at the time of loading.

Bottom-up transverse cracking can develop when truck loads are located near the centre of a panel at times

*Corresponding author. Email: jmv7@pitt.edu

ISSN 1029-8436 print/ISSN 1477-268X online

DOI: 10.1080/10298436.2010.489113
http://www.informaworld.com

when large positive effective temperature gradients are present through the slab (i.e. the top of the slab is warmer than the bottom of the slab). The resulting environment-related loss of support at mid-slab leads to higher stresses and more rapid accumulation of fatigue damage at the bottom of the slab under the wheel loads. Top-down transverse cracking develops more rapidly when a large negative effective temperature gradient is present (i.e. the top of the slab is cooler than the bottom of the slab, resulting in loss of support at the slab edges and corners) and heavy axle loads are applied simultaneously to each end of the slab. In the MEPDG models, the total transverse cracking in JPCP (in terms of per cent cracked slabs) is obtained by adding percentages of predicted bottom-up and top-down slab cracking and subtracting the probability that both occur in the same panel.

For the design procedure just described, it is essential to accurately characterise the shape of the slab at the time the load is applied. This requires determining the built-in gradient, as well as the temperature and moisture distributions through the slab thickness at the time of loading. In the MEPDG, the transient, often nonlinear temperature distribution through the slab is predicted at every hour of the pavement life using the EICM (McCracken *et al.* 2008). An equivalent linear temperature difference, $\Delta T_{\text{transient}}$, is obtained based on an equivalent stress condition (ARA, Inc., ERES Division 2004). The transient moisture distribution attributed to reversible shrinkage in the upper 50 mm of the slab is determined on a monthly basis in the MEPDG analysis; the equivalent moisture-related temperature difference is determined by matching slab stress conditions and is added to (or subtracted from) $\Delta T_{\text{transient}}$ to obtain an effective $\Delta T_{\text{transient}}$ that accounts for both temperature and reversible moisture effects. The contribution of the built-in temperature difference, $\Delta T_{\text{built-in}}$, is equally important, but is more difficult to determine (Well *et al.* 2006).

When concrete pavements first begin to set and harden, they are in full contact with the foundation (i.e. they are 'flat') and are in a zero-stress condition (even when in the presence of temperature and/or moisture gradients) because the concrete is just leaving a plastic state. Figure 1(a) shows how a positive temperature difference or gradient can be developed in the slab if paving takes place during the morning hours and setting and hardening take place on a sunny afternoon when the solar radiation is intense, causing the temperature at the top of the slab to increase above that at the slab bottom. When the concrete slab sets under these temperature conditions, a negative temperature difference is 'built into the slab' and the slab will curl upwards as if a negative temperature gradient is present when the actual temperature difference between the top and the bottom of the slab is zero. Figure 1(b) illustrates this point by showing how a transient temperature difference of 0°C will cause the example slab to curl upwards, as if an equivalent temperature difference of −5.5°C was applied. Previous studies have shown $\Delta T_{\text{built-in}}$ to be critical to JPCP-predicted performance using the MEPDG (Hall and Beam 2004; Barenberg *et al.* 2005; Coree 2005; Kannekanti and Harvey 2005; Gutierrez 2008; Khazanovich *et al.* 2008).

MEPDG v1.0 allows the user to assign an input value for the built-in temperature difference based on local knowledge/information. Many factors affect the magnitude of the actual value of $\Delta T_{\text{built-in}}$, including the characteristics of the concrete (e.g. cement content, set time and the heat of hydration generated), slab thickness, construction practices, initial concrete temperature and ambient climatic conditions during and after paving. Several approaches to determine $\Delta T_{\text{built-in}}$ are reported in the literature (Yu *et al.* 1998; Byrum 2000; Beckemeyer *et al.* 2002; Rao and Roesler 2005; Well *et al.* 2006).

It should be noted that the value of $\Delta T_{\text{built-in}}$ used in the MEPDG is intended to account not only for the temperature and moisture gradients in the slab at the time the slab sets, but also for the irreversible component of the concrete drying shrinkage over time, concrete creep and slab support or settlement into the subbase (Khazanovich *et al.* 2001; Khazanovich and Yu 2005). Since there was no formal procedure for determining a value for $\Delta T_{\text{built-in}}$ that accounted for all of these factors when the MEPDG was developed, a single standard value for $\Delta T_{\text{built-in}}$ (−5.5°C) was determined during the calibration of the MEPDG to minimise the differences between predicted and observed distresses (residual prediction errors). This value was recommended for general use in pavement design and is the default value provided in the MEPDG. As a result, MEPDG users must choose between using an actual site-specific

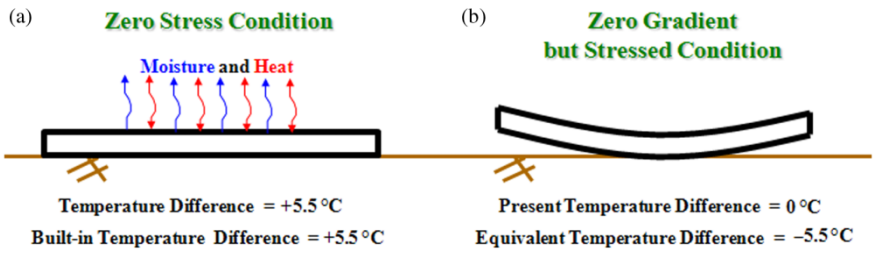

Figure 1. Illustration of effective built-in temperature difference.

value for $\Delta T_{\text{built-in}}$ and a default value that was established during the model calibration process.

Since the default value for $\Delta T_{\text{built-in}}$ was developed as a part of the MEPDG calibration process, it is reasonable to expect that its use will provide good predictions for the cracking of JPCP projects that are within the inference space of the MEPDG calibration database. Furthermore, recent studies by Vandenbossche *et al.* (2009) suggest that using the default input value for $\Delta T_{\text{built-in}}$ also closely predicts the performance of at least some JPCP projects that are outside of the inference space of the MEPDG calibration database. No published studies to date, however, have examined the implications of using a single default value for $\Delta T_{\text{built-in}}$ on MEPDG cracking predictions in general or have examined if $\Delta T_{\text{built-in}}$ is properly accounted for within the MEPDG framework. Therefore, this study was designed with these objectives in mind.

To accomplish these goals, the MEPDG-predicted cracking damage was determined for a range of values of $\Delta T_{\text{built-in}}$ for a specified JPCP in different climates (with resulting different distributions of $\Delta T_{\text{transient}}$). The next step was to evaluate the effects of the various factors that influence predicted cracking with changes in $\Delta T_{\text{built-in}}$. Factors considered include: combinations of $\Delta T_{\text{transient}}$ and $\Delta T_{\text{built-in}}$ for different climates; time of day of traffic loading in different climates; and varying slab thickness and joint spacing under constant environmental and traffic conditions.

3. Effect of climatic conditions

Large and rapid changes in ambient temperatures generally result in the development of large transient temperature gradients or differences in pavement slabs. Stresses due to an effective $\Delta T_{\text{built-in}}$ will either add to or subtract from the stresses due to effective $\Delta T_{\text{transient}}$, depending upon their respective signs (positive or negative). Therefore, the value of $\Delta T_{\text{built-in}}$ that minimises the development of JPCP cracking distress should vary as a function of the effective $\Delta T_{\text{transient}}$ (accounting for both transient temperature and reversible moisture effects) as well as the slab geometry and material properties. (Recall that irreversible shrinkage warping is accounted for by the effective $\Delta T_{\text{built-in}}$.)

The most intuitive approach for evaluating the response of the model to the effective $\Delta T_{\text{built-in}}$ is to evaluate the predicted behaviour of a single pavement design for several sites that represent significantly different climatic conditions such that different magnitudes and distributions of effective $\Delta T_{\text{transient}}$ will be considered. If $\Delta T_{\text{built-in}}$ is truly a design input variable and not effectively a calibration constant, then one would expect that the value of $\Delta T_{\text{built-in}}$ that minimises predicted JPCP fatigue damage and slab cracking will vary between sites.

The first step in this study was to identify locations in the USA representing a range of climatic conditions for which sufficient climatic data were available. The following sites were selected: Pittsburgh (Pennsylvania), Phoenix (Arizona), Miami (Florida), Wichita (Kansas), Aspen (Colorado) and Atlanta (Georgia). Figure 2 presents the frequency distribution of daily ambient temperature ranges for these six different locations based on a minimum of 7 years of climatic data (obtained from National Oceanic and Atmospheric Administration (2007)). Figure 2 shows that climatic conditions vary considerably among these sites, from Miami, which exhibits the smallest average daily temperature fluctuations, to Aspen, which exhibits the largest temperature swings.

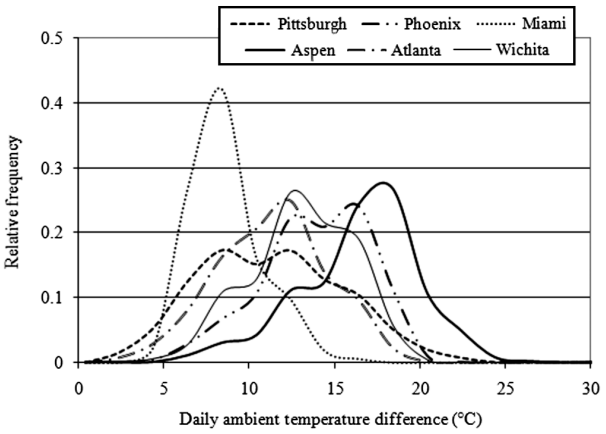

Figure 2. Frequency distribution of daily ambient temperature differences for six sites.

The EICM in the MEPDG was used to determine the magnitude of equivalent $\Delta T_{\text{transient}}$ that develops in a reference JPCP pavement design due to the climate at these six locations. Table 1 describes the pavement structure, materials and design traffic for the reference JPCP used in this analysis. MEPDG default values were used for all other design and traffic inputs.

Figure 3 presents the frequency distribution curves for the MEPDG/EICM-computed $\Delta T_{\text{transient}}$ in the reference JPCP at each of the selected sites. The distributions for Wichita, Atlanta and Pittsburgh are similar, with median $\Delta T_{\text{transient}}$ values occurring between -3 and -4°C. The Miami climate results in a similar median $\Delta T_{\text{transient}}$ (-4°C), but the variability of $\Delta T_{\text{transient}}$ is higher at this site, with generally lower temperature differences than that are predicted for the other sites. The largest median $\Delta T_{\text{transient}}$ values were computed for the reference pavement sections in Aspen and Phoenix (-8 and -7°C, respectively). Comparison of Figures 2 and 3 shows that $\Delta T_{\text{transient}}$ values are generally higher for the sites with higher daily temperature fluctuations (i.e. Aspen and Phoenix), which is expected.

Figure 3 shows that the maximum predicted positive $\Delta T_{\text{transient}}$ values are larger than the maximum predicted negative $\Delta T_{\text{transient}}$ values for all locations; however, negative $\Delta T_{\text{transient}}$ values are predicted to occur more

Table 1. Summary of MEPDG reference design inputs.

Design life	20 years
Traffic	
Initial two-way annual average daily truck traffic	2000
Number of lanes in design direction	2
Percentage of trucks in design direction (%)	50
Percentage of trucks in design lane (%)	95
Growth rate	No growth
Structure – design features	
Permanent curl/warp (°C)	Variable
Structure – layers	
Layer 1 – JPCP	
General properties	
PCC material	JPCP
Layer thickness (mm)	254
Unit weight (kg/m^3)	2400
Poisson's ratio	0.2
Strength properties	
Input level	Level 3
28-day PCC modulus of rupture (MPa)	4.1
28-day PCC compressive strength (MPa)	n/a
Layer 2 – unbound material	
Material type	A-3
Layer thickness (mm)	130
Layer 3 – unbound material	
Unbound material	A-3
Thickness (mm)	Semi-infinite

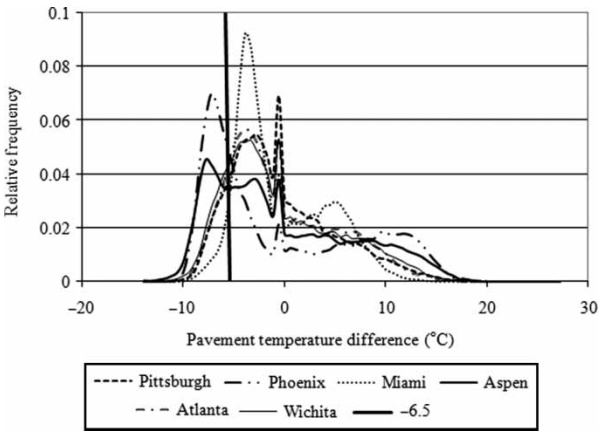

Figure 3. Frequency distribution of daily temperature differences in slabs for reference pavement design at six different sites.

frequently than positive values. This is important to note because the effects of temperature and moisture gradients on JPCP slab cracking are affected by both the magnitude and frequency of the gradients.

Key descriptors for the $\Delta T_{transient}$ distributions shown in Figure 3 are summarised in Table 2. It is interesting to note that, in spite of the obvious climatic differences at each site, the predicted values of $\Delta T_{transient}$ for all sites are positive about 40% of the time and negative about 60% of the time. In addition, the mean value of $\Delta T_{transient}$ is about -0.4°C for all of the sites. It can also be seen that there is a secondary frequency peak at -0.6°C for all sites, which is difficult to explain and may represent a problem with the integration of the EICM in the MEPDG.

Table 2. Summary of key frequency distribution descriptors from Figure 3.

Location	Primary peak (°C)	Secondary peak (°C)	Average (°C)	% < 0°C	% > 0°C
Miami	−3.9	−0.6	−0.4	60	40
Aspen	−7.8	−0.6	−0.3	60	40
Wichita	−3.9	−0.6	−0.4	61	39
Phoenix	−7.2	−0.6	−0.3	60	40
Atlanta	−3.9	−0.6	−0.4	61	39
Pittsburgh	−2.8	−0.6	−0.4	61	39

The next step is to relate these temperature differentials to fatigue damage in the slab. The accumulation of fatigue damage for slab cracking should be minimised when the effective $\Delta T_{transient}$ at the time of loading is equal to (and of opposite sign to) the effective $\Delta T_{built\text{-}in}$ because the slabs should be flat and fully supported under these conditions. This relationship between fatigue damage and $\Delta T_{built\text{-}in}$ can be verified by running the MEPDG software using the reference input data for this study for the selected pavement study sites while varying $\Delta T_{built\text{-}in}$. The value for $\Delta T_{built\text{-}in}$ that minimises fatigue damage can be considered to be the 'optimal' value for $\Delta T_{built\text{-}in}$ at a given site. The results of this analysis are tabulated in Table 3, which presents computed fatigue damage (for top-down cracking, bottom-up cracking and total damage) and predicted slab cracking for various assumed values of $\Delta T_{built\text{-}in}$. Figure 4 presents the observed relationships between predicted cracking and assumed $\Delta T_{built\text{-}in}$ for the six study sites.

One would expect that different values of $\Delta T_{built\text{-}in}$ would be required to minimise predicted cracking at sites with significantly different climates. Figure 3 shows that the magnitude and frequency distribution of $\Delta T_{transient}$ varies significantly between sites. However, Table 3 and Figure 4 suggest that, for the reference pavement design and traffic summarised in Table 1, there is a nearly constant value of $\Delta T_{built\text{-}in}$ (approximately -6.5°C) that minimises the MPEDG-computed fatigue damage and resulting transverse cracking for all of the sites considered. This value is quite close to the recommended MEPGD default input value of -5.5°C. This finding suggests that the MEPDG predicts minimum JPCP fatigue and cracking at a non-site-dependent constant of -6.5°C for normal traffic loading conditions at the sites considered in this study.

It can also be seen from Table 3 that the predominant fatigue mode is for top-down cracking when $\Delta T_{built\text{-}in}$ is more negative than the -6.5°C value that minimises damage. The predominant fatigue mode is for bottom-up cracking when $\Delta T_{built\text{-}in}$ is less negative than -6.5°C

Table 3. Summary of built-in temperature difference analysis at different sites.

Site		Built-in temperature difference (°C)								
		−9.0	−8.0	−7.0	*−6.5*	−6.0	−5.5	−5.0	−4.5	−4.0
Pittsburgh, PA	FDb-u	0.010	0.014	0.02	*0.000*	**0.037**	**0.051**	**0.069**	**0.094**	**0.126**
	FDt-d	**0.053**	**0.036**	**0.023**	*0.015*	0.01	0.007	0.005	0.003	0.002
	FD_{total}	0.063	0.049	0.043	*0.015*	0.047	0.058	0.074	0.097	0.128
	TCRACK	0.3	0.2	0.1	*0.1*	0.2	0.3	0.5	0.9	1.6
Phoenix, AZ	FDb-u	0.027	0.039	0.054	*0.077*	**0.107**	**0.148**	**0.205**	**0.28**	**0.382**
	FDt-d	**0.231**	**0.163**	**0.114**	*0.078*	0.058	0.043	0.031	0.022	0.016
	FD_{total}	0.258	0.202	0.168	*0.155*	0.166	0.191	0.237	0.302	0.398
	TCRACK	5.3	2.8	1.6	*1.3*	1.5	2.4	4.3	7.5	13.0
Miami, FL	FDb-u	0.001	0.001	0.002	0.003	*0.004*	*0.006*	**0.009**	**0.012**	**0.018**
	FDt-d	**0.030**	**0.019**	**0.012**	**0.008**	*0.005*	*0.003*	0.002	0.001	0.001
	FD_{total}	0.031	0.020	0.014	0.010	*0.009*	*0.009*	0.011	0.014	0.019
	TCRACK	0.1	0.0	0.0	0.0	*0.0*	*0.0*	0.0	0.0	0.0
Wichita, KS	FDb-u	0.006	0.009	0.017	*0.024*	**0.034**	**0.047**	**0.051**	**0.073**	**0.098**
	FDt-d	**0.101**	**0.068**	**0.035**	*0.022*	0.016	0.011	0.010	0.007	0.004
	FD_{total}	0.107	0.077	0.051	*0.047*	0.049	0.058	0.061	0.079	0.102
	TCRACK	1.1	0.5	0.2	*0.1*	0.1	0.3	0.3	0.6	1.0
Aspen, CO	FDb-u	0.031	0.045	0.047	*0.067*	**0.092**	**0.125**	**0.187**	**0.244**	**0.327**
	FDt-d	**0.256**	**0.193**	**0.102**	*0.073*	0.057	0.043	0.051	0.039	0.029
	FD_{total}	0.279	0.229	0.149	*0.139*	0.149	0.168	0.228	0.273	**0.347**
	TCRACK	6.4	3.9	1.3	*1.0*	*1.2*	1.8	3.8	5.9	9.9
Atlanta, GA	FDb-u	0.004	0.006	0.013	*0.018*	**0.025**	**0.035**	**0.033**	**0.047**	**0.064**
	FDt-d	**0.072**	**0.048**	**0.026**	*0.016*	0.012	0.008	0.006	0.004	0.003
	FD_{total}	0.076	0.053	0.039	*0.034*	0.037	0.043	0.040	0.051	**0.067**
	TCRACK	0.5	0.3	0.1	*0.1*	0.1	0.1	0.1	0.2	0.4

Notes: FD, fatigue damage; b-u, bottom-up; t-d, top-down; TCRACK, transverse crack. Bold values indicate the predominant mode of fatigue damage. Italicised values indicate the minimised fatigue damage or transverse cracking.

or is positive. The predominance of top-down cracking for highly negative values of $\Delta T_{\text{built-in}}$ is not unexpected, but the computed values do not shed light on why $\Delta T_{\text{built-in}} = -6.5$°C seems to minimise JPCP transverse cracking irrespective of the climate.

The amounts of cracking that are predicted to develop with changes in the MEPDG input $\Delta T_{\text{built-in}}$ are presented in Figure 4. The cracking predicted for the reference pavement at the Miami site is less sensitive to changes in $\Delta T_{\text{built-in}}$ than is the cracking at the other sites, as indicated by the large range of $\Delta T_{\text{built-in}}$ values for this site where predicted cracking is zero. The Aspen and Phoenix sites present the most sensitivity to $\Delta T_{\text{built-in}}$. Recalling (from Figure 3) that the Miami site generally resulted in the smallest $\Delta T_{\text{transient}}$ values and that Aspen and Phoenix generally produced the largest values, there appears to be a correlation between the frequency distribution for $\Delta T_{\text{transient}}$ and the sensitivity to input values of $\Delta T_{\text{built-in}}$ (in terms of predicted JPCP fatigue damage and cracking).

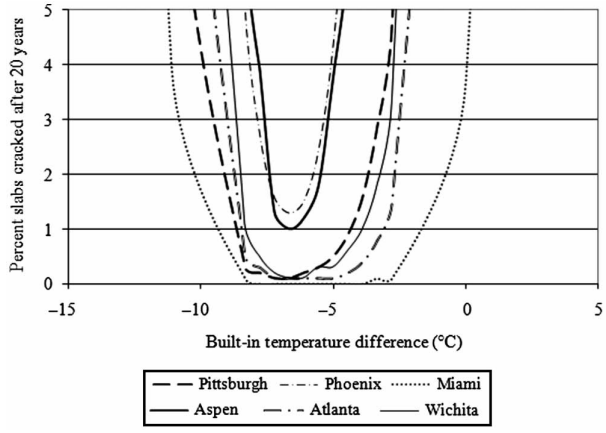

Figure 4. Predicted cracking as a function of assumed built-in temperature difference at six sites.

It is also interesting to observe in Figure 4 that the rates of increase in predicted cracking with changes in the input value of $\Delta T_{\text{built-in}}$ appear to be comparable at any given site, regardless of whether the increase in cracking is due to more negative values of $\Delta T_{\text{built-in}}$ (i.e. bottom-up damage) or less negative values (i.e. top-down damage). This is somewhat unexpected because the frequency distributions of $\Delta T_{\text{transient}}$ presented in Figure 3 appear to be rather skewed and not at all the symmetrical normal distribution one might associate with such behaviour.

4. Influence of hourly traffic distribution

One factor that might help explain why the value of $\Delta T_{\text{built-in}}$ that minimises predicted cracking does not appear to be sensitive to the site-specific climatic conditions is the

Table 4. Assumed hourly traffic distributions for night-time and daytime loading conditions.

More traffic during daytime				More traffic at night			
Hour (am)	Traffic (%)	Hour (pm)	Traffic (%)	Hour (am)	Traffic (%)	Hour (pm)	Traffic (%)
12	2.3	12	5.9	12	5.9	12	3.1
1	2.3	1	5.9	1	5.9	1	3.1
2	2.3	2	5.9	2	5.9	2	2.3
3	2.3	3	5.9	3	5.9	3	2.3
4	2.3	4	4.6	4	5.9	4	2.3
5	2.3	5	4.6	5	5.9	5	2.3
6	5	6	4.6	6	4.6	6	2.3
7	5	7	4.6	7	4.6	7	2.3
8	5	8	3.1	8	4.6	8	5
9	5	9	3.1	9	4.6	9	5
10	5.9	10	3.1	10	3.1	10	5
11	5.9	11	3.1	11	3.1	11	5

consideration of the time of the day the pavement is being loaded by traffic. The preceding analysis was performed assuming that 64% of the traffic was applied between 8 am and 7 pm, times when positive transient temperature differences tend to be present, partially (or wholly) offset by the negative built-in temperature differences and resulting in flatter slabs during loading with less resultant JPCP fatigue damage and cracking.

The influence of the hourly traffic distribution on the value of $\Delta T_{\text{built-in}}$ that minimises predicted JPCP cracking can be observed by shifting the daily distribution of traffic. To accomplish this, the MEDPG default hourly traffic distribution (which was used for the previous analysis and is presented in Table 4 and displayed graphically in Figure 5) was shifted by − 10 h (also as presented in Table 4 and Figure 5) to establish a heavier influence for night-time loadings. The damage and cracking predicted by the MEPDG for reference pavement at the Pittsburgh site for these two loading conditions and a range of $\Delta T_{\text{built-in}}$ values is summarised in Table 5 and Figure 6.

Table 5 shows the summary of the results from this analysis. As described previously, the value for $\Delta T_{\text{built-in}}$ that minimised the accumulation of JPCP fatigue and cracking was − 6.5°C when the traffic loading was more heavily concentrated during the daytime. This value shifts slightly to − 5.5°C when the traffic loading is more heavily concentrated during the night-time when $\Delta T_{\text{transient}}$ is more likely to be negative and additive with $\Delta T_{\text{built-in}}$. It is noteworthy that there is so little difference in the values of $\Delta T_{\text{built-in}}$ that minimise the predicted JPCP fatigue and cracking for these different traffic loading distributions.

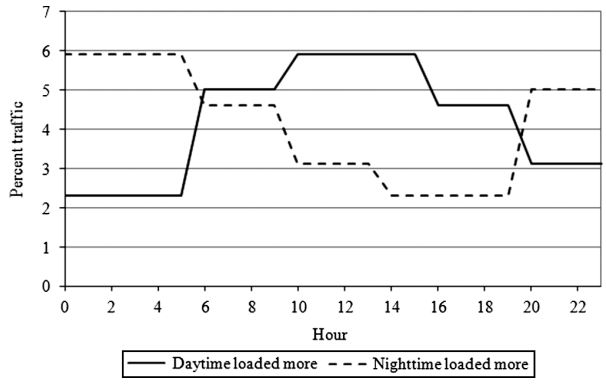

Figure 5. Assumed hourly traffic distributions for daytime loading and night-time loading.

To further evaluate the effects of the time of loading, all traffic was assumed to be applied during a single hour (representing the highest positive or negative transient temperature difference conditions). The times selected for consideration were 2 pm (when a positive gradient is present in the slab) and 3 am (when a negative gradient is present).

Table 6 and Figures 7–9 summarise the results of these analyses and show that the value of $\Delta T_{\text{built-in}}$ that minimises predicted JPCP fatigue and cracking at the Pittsburgh site is − 11°C for daytime loading and 0°C for night-time loading. These values are significantly different from each other and from the value that results when the complete spectra of expected temperature differences and traffic load distributions are used. In other words, a large negative $\Delta T_{\text{built-in}}$ (exceeding − 11°C) is required to overcome the large positive gradients that develop at 2 pm in the afternoon, while the combined effects of the transient temperature gradient and moisture differences (due to reversible shrinkage) present in the slab at 3 am appear to be greater than − 5.5°C. The latter case is indicated by the limited top-down damage that occurs at an assumed $\Delta T_{\text{built-in}}$ of 5.5°C. The MEPDG limits the range of the built-in equivalent temperature difference to less than 5.5°C so a broader range of values could not be evaluated.

The predicted cracking for the Pittsburgh site under time-concentrated loading shows the trends that would be anticipated. By forcing the application of all traffic loads within extreme conditions of $\Delta T_{\text{transient}}$, the value of $\Delta T_{\text{built-in}}$ that minimises predicted JPCP fatigue and cracking changes significantly.

Table 5. Summary of built-in temperature difference analysis results for different loading times.

	Built-in temperature difference (°C)									
Pittsburgh	−16.5	−14.0	−11.0	−8.5	−6.5	−5.5	−3.0	0.0	3.0	5.5
Daytime										
FDb-u	0.000	0.000	0.002	0.010	*0.030*	**0.051**	**0.222**	**0.834**	**2.656**	**7.371**
FDt-d	**3.499**	**1.320**	**0.317**	**0.053**	*0.010*	0.007	0.001	0.000	0.000	0.000
FD_{total}	3.499	1.320	0.319	0.063	*0.040*	0.058	0.223	0.834	2.656	7.371
Crack	92.3	63.4	9.3	0.3	*0.1*	0.3	4.8	41.1	87.4	98.1
Night-time										
FDb-u	0.000	0.000	0.001	0.004	0.010	*0.022*	**0.101**	**0.377**	**1.217**	**3.427**
FDt-d	**5.295**	**2.079**	**0.522**	**0.095**	**0.030**	*0.013*	0.001	0.000	0.000	0.000
FD_{total}	5.295	2.079	0.522	0.095	0.040	*0.035*	0.102	0.377	1.217	3.427
Crack	96.4	81.0	21.6	0.9	0.1	*0.1*	1.1	12.7	59.6	92.0

Note: For description of the bold and italicised values, see Table 3.

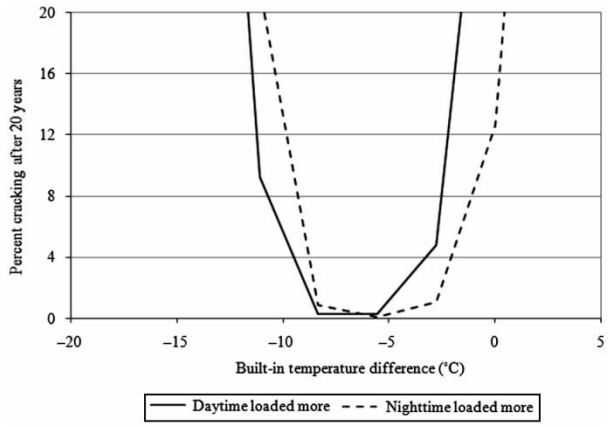

Figure 6. Predicted cracking vs. built-in temperature difference for day and night loading conditions at the Pittsburgh site.

A similar analysis was performed for the Aspen test site; the results of this analysis are presented in Table 7 and Figures 10–12. The value of $\Delta T_{built\text{-}in}$ that minimises predicted JPCP fatigue and slab cracking for the Aspen site under these conditions is computed as being −14 and 0°C for daytime and night-time loadings, respectively. As with the Pittsburgh site, the difference is quite significant. It can also be noted that the crack-minimising value of $\Delta T_{built\text{-}in}$ for night-time loading for the reference pavement is slightly different for the two sites (−11 vs. −14°C for Pittsburgh and Aspen, respectively). This difference is not unexpected because the maximum positive temperature difference that develops in the reference pavement for the Aspen location is higher than that at the Pittsburgh location. The minimising value for $\Delta T_{built\text{-}in}$ for night-time loading is similar for the two sites, which may or may not be reasonable.

5. Effect of varying slab thickness

As slab thickness changes, $\Delta T_{transient}$ values can be expected to change and the slab response to both environmental and applied loads changes as well, perhaps resulting in different values of $\Delta T_{built\text{-}in}$ that minimise the development of slab cracking.

In this study, the value of $\Delta T_{built\text{-}in}$ that minimises predicted JPCP fatigue and cracking was determined for slabs at the Pittsburgh site with thicknesses of 178, 254 and 330 mm. The frequency distribution curves for $\Delta T_{transient}$ for these thicknesses (as computed by the MEPDG/EICM module) are provided in Figure 13, which shows that the median value for $\Delta T_{transient}$ is about −3°C for all three slab

Table 6. Built-in temperature difference analysis for loading at specific hours in Pittsburgh.

	Built-in temperature difference (°C)									
Pittsburgh	−19.5	−14.0	−11.0	−8.5	−6.5	−5.5	−3.0	0.0	3.0	5.5
Traffic 100% at 2 pm										
FDb-u	0.000	0.001	*0.007*	**0.042**	**0.115**	**0.215**	**0.922**	**3.330**	**10.105**	**25.929**
FDt-d	**0.713**	**0.064**	*0.010*	0.001	0.001	0.000	0.000	0.000	0.000	0.000
FD_{total}	0.713	0.065	*0.017*	0.043	0.115	0.216	0.922	3.330	10.105	25.929
Crack	33.8	0.4	*0.0*	0.2	1.4	4.6	46.0	91.5	99.0	99.8
Traffic 100% at 3 am										
FDb-u	0.000	0.000	0.000	0.000	0.000	0.000	0.000	*0.001*	**0.007**	**0.048**
FDt-d	**12.027**	**2.907**	**0.748**	**0.134**	**0.039**	**0.019**	**0.002**	*0.000*	0.000	0.000
FD_{total}	12.027	2.907	0.748	0.134	0.039	0.019	0.002	*0.001*	0.007	0.048
Crack	99.3	89.2	36.0	1.8	0.2	0.0	0.0	*0.0*	0.0	0.2

Note: For description of the bold and italicised values, see Table 3.

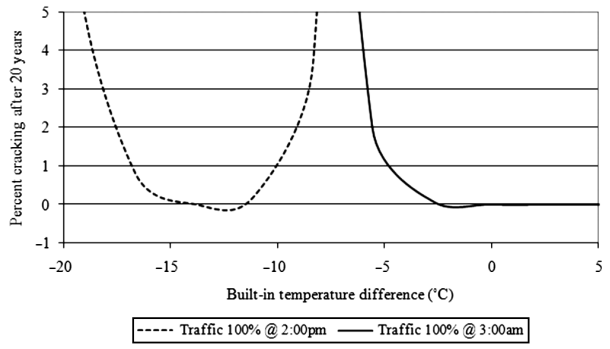

Figure 7. Predicted cracking vs. built-in temperature difference for pure (concentrated) day and night loading conditions at the Pittsburgh site.

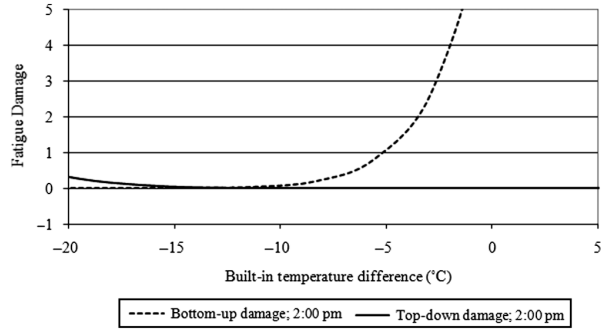

Figure 8. Predicted fatigue damage vs. built-in temperature difference for concentrated daytime traffic loading in Pittsburgh.

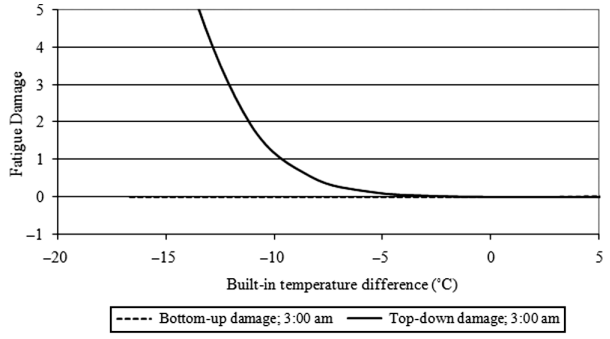

Figure 9. Predicted fatigue damage vs. built-in temperature difference for concentrated night-time traffic loading in Pittsburgh.

thicknesses, but that the range of values generally increases with increasing slab thickness (i.e. thicker slabs develop greater temperature differences). Figure 13 also shows the same secondary peak value of -0.6°C that was noted previously and that appears to be an indication of an error of some sort in the EICM as it is embedded in the MEPDG. This set of $\Delta T_{transient}$ distribution curves provides an opportunity to look at the effects of slabs with the same median $\Delta T_{transient}$ but differences in the magnitude and frequency of occurrence in the peak gradients on values of $\Delta T_{built\text{-}in}$ that minimise predicted JPCP fatigue and cracking.

The value of $\Delta T_{built\text{-}in}$ that minimises cracking was determined for each slab thickness for three different loading conditions: (1) MEPDG default hourly traffic distribution; (2) all traffic loads applied at 2 pm; and (3) all traffic loads applied at 3 am. All other MEPDG inputs were the same as previously defined.

A summary of the results of this analysis is provided in Table 8. It does appear that the crack-minimising values of $\Delta T_{built\text{-}in}$ become increasingly negative with decreasing slab thickness, especially when the traffic is distributed over a period of time (e.g. MEPDG default traffic distribution over time) and not concentrated in a single-hour time period (e.g. 2 pm or 3 am). This seems to indicate a possible problem in the treatment of $\Delta T_{built\text{-}in}$ in the MEPDG because larger temperature differences were shown to develop in the thicker slabs yet values of $\Delta T_{built\text{-}in}$ that minimise predicted fatigue and cracking tend to be less negative for these thicker slabs. If the results from these three slab thicknesses in Pittsburgh are compared with the results obtained for the reference slab in the Aspen climate using default traffic load distributions, it appears that varying slab thicknesses within the same climate has an effect on the crack-minimising value of $\Delta T_{built\text{-}in}$, but that the values are about the same for slabs with the same thickness being modelled in two different climates. This again raises questions concerning whether $\Delta T_{built\text{-}in}$ (as it has been developed and implemented in the MEPDG) is truly a site-specific user-defined study variable or is effectively a calibration constant for sites with normal traffic distributions.

It appears that the transient climatic conditions in the Pittsburgh slab model remain relatively constant for varying slab thicknesses when all loads are applied in a given time slot (e.g. 2 pm or 3 am). This is indicated by the fact that the crack-minimising $\Delta T_{built\text{-}in}$ values are similar for the various pavement thickness designs in Pittsburgh, but are drastically different from the value obtained for the Aspen test section.

6. Effect of varying joint spacing

Joint spacing is another factor that affects the stress and consequently fatigue damage caused by traffic loadings on curled slabs. An analysis was carried out to evaluate the minimising built-in temperature difference for pavements with different joint spacings (3.7 and 4.6 m) but the same thickness (254 mm) under Pittsburgh climatic conditions. The results are summarised in Table 9. The predicted cracking for each built-in temperature difference is much larger for longer slabs. However, the change in joint spacing does not affect the minimising built-in temperature difference.

7. Effect of transient moisture conditions in the slab

Another factor to consider is the effect of transient moisture conditions on the crack-minimising value for

Table 7. Built-in temperature difference analysis for loading at specific hours in Aspen.

Aspen	Built-in temperature difference (°C)									
	−22.0	−19.5	−14.0	−11.0	−8.5	−5.5	−3.0	0.0	3.0	5.5
100% at 2 pm										
FDb-u	0.000	0.000	*0.006*	**0.038**	**0.194**	**0.813**	**2.788**	**8.633**	**22.257**	**51.082**
FDt-d	**0.612**	**0.259**	*0.016*	0.002	0.000	0.000	0.000	0.000	0.000	0.000
FD_{total}	0.612	0.259	*0.022*	0.040	0.194	0.813	2.788	8.633	22.257	51.082
Crack	27.4	6.4	*0.0*	0.200	3.7	39.9	88.4	98.6	99.8	100.0
100% at 3 am										
FDb-u	–	–	0.000	0.000	0.000	0.000	0.000	*0.000*	**0.001**	**0.010**
FDt-d	–	–	**5.715**	**1.958**	**0.554**	**0.140**	**0.032**	*0.005*	0.000	0.000
FD_{total}	–	–	5.715	1.958	0.554	0.140	0.032	*0.005*	0.002	0.010
Crack	–	–	96.9	79.1	23.7	2.0	0.1	*0.0*	0.0	0.0

Note: For description of the bold and italicised values, see Table 3.

$\Delta T_{\text{built-in}}$. The MEPDG accounts for the reversible shrinkage in the concrete by calculating an equivalent linear temperature gradient as a function of the ambient relative humidity using Equation (1).

$$\text{ETG}_{\text{SH}i} = 3\cdot(\varphi\cdot\varepsilon_{\text{su}})\cdot(S_{\text{h}i} - S_{\text{h ave}})\cdot h_{\text{s}}\cdot\left(\frac{h}{2} - \frac{h_{\text{s}}}{3}\right)\Big/(\alpha\cdot h^2\times 100) \quad (1)$$

$$\varepsilon_{\text{su}} = C_1\cdot C_2\cdot\{0.02w^{2.1}(f'_{\text{c}})^{-0.28} + 270\} \quad (2)$$

$$S_{\text{h}i} = \begin{cases} 1.1\cdot\text{RH}_{\text{a}} & \text{RH}_{\text{a}} < 30\% \\ 1.4 - 0.01\cdot\text{RH}_{\text{a}} & 30\% < \text{RH}_{\text{a}} < 80\% \\ 3.0 - 0.03\cdot\text{RH}_{\text{a}} & \text{RH}_{\text{a}} > 80\% \end{cases} \quad (3)$$

where $\text{ETG}_{\text{SH}i}$ is the equivalent ΔT of the change in moisture warping in month i; expressed in °C; φ is the reversible shrinkage factor as a fraction of total shrinkage

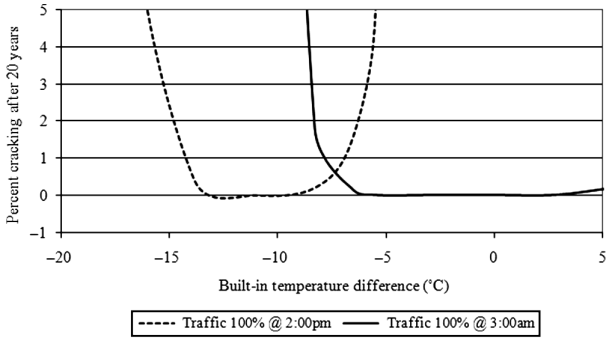

Figure 10. Predicted cracking vs. built-in temperature difference for pure (concentrated) day and night loading conditions at the Aspen site.

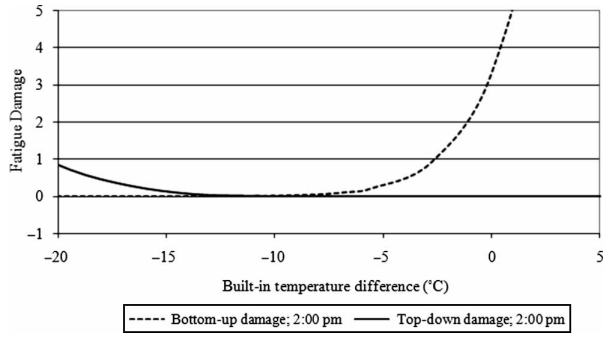

Figure 11. Predicted fatigue damage vs. built-in temperature difference for concentrated daytime traffic loading in Aspen.

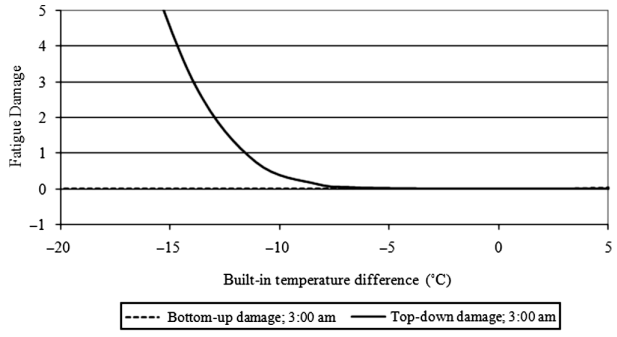

Figure 12. Predicted fatigue damage vs. built-in temperature difference for concentrated night-time traffic loading in Aspen.

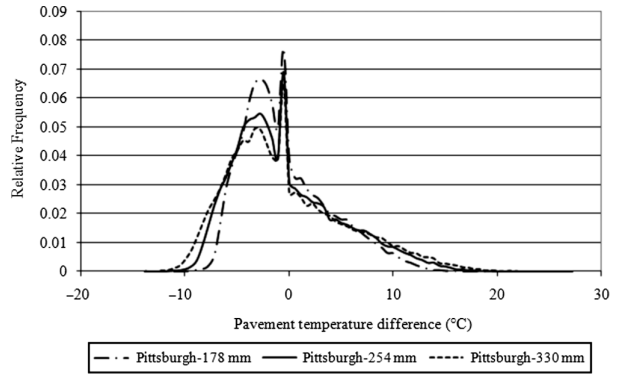

Figure 13. Frequency distribution of transient temperature difference for slabs of various thicknesses in Pittsburgh.

Table 8. Summary of the crack-minimising built-in gradients for a range of slab thicknesses.

	Time when traffic is applied		
Location/slab thickness	MEPDG default	2 pm	3 am
Pittsburgh/178 mm	−8	−11	−2
Pittsburgh/254 mm	−6.5	−11	0
Pittsburgh/330 mm	−5	−9	0
Aspen/254 mm	−6.5	−14	0

(default = 0.5); ε_{su} is the ultimate shrinkage (mm/mm × 10^{-6}) and can be estimated using Equation (2); C_1 is the cement type constant (1.0 for type I); C_2 is the curing compound constant (1.2 when the curing compound is used); w is the water content in the concrete mix, kg/m^3; f'_c is the 28-day compressive strength, MPa; S_{hi} is the relative humidity factor for month i, calculated using Equation (3); RH_a is the ambient average relative humidity, per cent; h_s is the depth of shrinkage zone (typically 50 mm); h is the Portland cement concrete (PCC) slab thickness, mm; and α is the PCC coefficient of thermal expansion, radians/°C.

The MEPDG assumes that the moisture condition within the slab is established by the average relative humidity and that the moisture content in the upper 50 mm of the slab fluctuates as a function of the monthly average relative humidity. The monthly average relative humidities for the Pittsburgh and Aspen sites were obtained from the MEPDG output files and are provided in Figure 14, which clearly shows that the average relative humidity is lower and fluctuates more in Aspen. These values, along with Equation (1), were used to determine the equivalent temperature differences for these moisture gradients ($\Delta T_{equiv\text{-}moist}$). The cumulative frequency plots for $\Delta T_{equiv\text{-}moist}$ for Pittsburgh and Aspen are provided in Figure 15, and are summarised in Table 10.

Figure 15 shows that the effect of the warping associated with reversible shrinkage, $\Delta T_{equiv\text{-}moist}$, ranges from −3 to +3°C in Aspen and −1.5 to 2.0°C in Pittsburgh, with median values that are near zero for both cities. While these values are relatively small, their impact could be significant for certain combinations of $\Delta T_{transient}$ and $\Delta T_{built\text{-}in}$ that produce rapid accumulation of JPCP fatigue damage.

An analysis was performed to further evaluate the relative contributions of each component of the total effective temperature difference [i.e. $\Delta T_{built\text{-}in}$ (considering temperature and moisture conditions at the time of set, along with irreversible drying shrinkage), $\Delta T_{transient}$ (hourly effective transient temperature difference) and $\Delta T_{equiv\text{-}moist}$ (effective temperature difference due to reversible moisture gradients)]. Figure 16 summarises the computed hourly equivalent linear temperature differences, $\Delta T_{transient}$, in July for a 330 mm slab constructed in Pittsburgh. The distribution of equivalent linear temperature differences that occur in July at 7 am are provided in Figure 17. This time was selected because the average effective temperature difference present is close to zero and the range of gradients that develop at this time (−2.2 to 5°C) is relatively small. The average $\Delta T_{equiv\text{-}moist}$ for July for this site was computed as −0.21°C. Therefore, the combined effective transient temperature difference that accounts for both temperature and moisture can be estimated as being between −2.4 and 4.8°C at 7 am in July at this site. With such a small effective temperature difference in the slab, it can be concluded that the slab is predicted (on average) to be relatively flat at 7 am during the month of July.

The crack-minimising value of $\Delta T_{built\text{-}in}$ at this time should be equal to the magnitude of (and of opposite sign to) the sum of $\Delta T_{transient} + \Delta T_{equiv\text{-}moist}$. To test this relationship, the MEPDG was used to perform an analysis with all traffic loads assumed to be applied at 7 am during the month of July. For this set of load and environmental conditions, very little damage was predicted for $\Delta T_{built\text{-}in}$ ranging between −14 and 2.5°C. The fact that very little damage is predicted when $\Delta T_{built\text{-}in}$ is −14°C is further support of concerns regarding the proper consideration of $\Delta T_{built\text{-}in}$ in the MEPDG.

Table 9. Summary of the minimising built-in gradients for different joint spacings.

	Built-in temperature difference (°C)					
Joint spacing (m)	−11	−8.5	−6.5	−5.5	−3	0
3.7						
FDb-u	0.000	0.002	*0.003*	**0.005**	**0.016**	**0.045**
FDt-d	**0.027**	**0.005**	*0.001*	0.001	0.000	0.000
FD_{total}	0.027	0.006	*0.004*	0.006	0.016	0.045
TCRACK	0.1	0	*0*	0	0	0.2
4.6						
FDb-u	0.002	0.010	*0.027*	**0.051**	**0.222**	**0.834**
FDt-d	**0.317**	**0.053**	*0.015*	0.007	0.001	0.000
FD_{total}	0.318	0.063	*0.041*	0.058	0.223	0.834
TCRACK	9.3	0.3	*0.1*	0.3	4.8	41.1

Note: For description of the bold and italicised values, see Table 3.

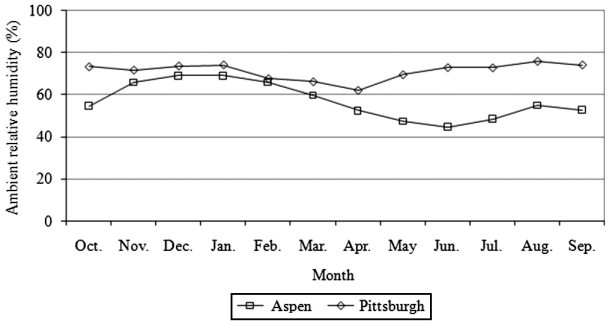

Figure 14. Average monthly relative humidity at Aspen and Pittsburgh sites.

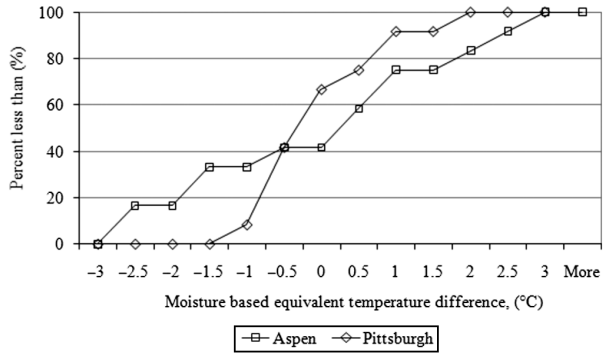

Figure 15. Cumulative frequency of moisture-based equivalent temperature difference at Aspen and Pittsburgh sites.

Table 10. Summary statistics for the reversible moisture-based equivalent temperature difference.

Location	50% of the time (°C)	Range (°C)	Average (°C)
Pittsburgh	0.5 to −0.75	−0.7 to 1.9	−0.5
Aspen	1.25 to −1.75	−2.5 to 2.7	0.03

A previous study has shown that using the default value of $\Delta T_{\text{built-in}}$ in the MEPDG results in much better estimations of the observed cracking than that are obtained using measured values (Vandenbossche *et al.* 2009). Therefore, at this time, it is recommended that the default value be used in all analyses until the MEPDG more realistically reflects the effects of $\Delta T_{\text{built-in}}$ on JPCP slab cracking.

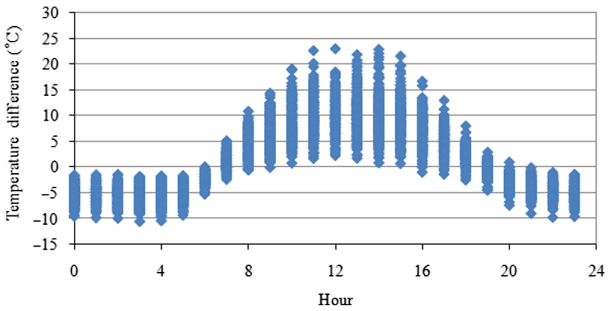

Figure 16. Daily transient slab temperature differences for 330 mm slab in Pittsburgh in July.

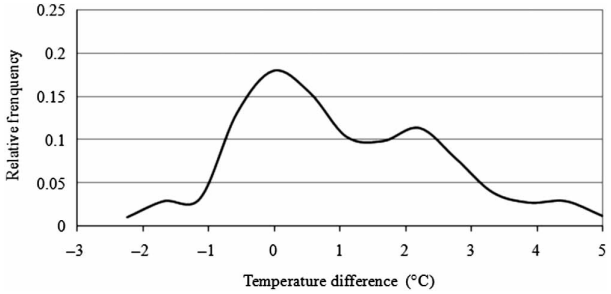

Figure 17. Distribution of transient slab temperature differences at 7 am in July in Pittsburgh.

8. Evaluating cracking prediction using field data

To validate the rationality of using a local built-in equivalent temperature difference rather than the default value, predictions are made with both temperature differences and compared with the observation on nine different cells in the 5- and 10-year mainline sections at Minnesota Road Research Facility (Mn/ROAD). The use of the pavement sections (test cells) constructed at

Table 11. Design of Mn/DOT test sections used for analysis.

Cell	Slab thickness (mm)	Joint spacing (m)	Lane widths, inside/outside (m)	Dowel diameter (mm)	Base/subbase[a]
5	190	6.1	4.0/4.3	25	80 mm cl4sp over 1730 mm cl3sp
6	185	4.6	4.0/4.3	25	130 mm cl4sp
7	195	6.1	4.0/4.3	25	100 mm PASB over 80 mm cl4sp
8	190	4.6	4.0/4.0/4.3	25	100 mm PASB over 80 mm cl4sp
9	195	4.6	4.0/4.0/4.3	25	100 mm PASB over 80 mm cl4sp
10	255	6.1	3.7/3.7	32	100 mm PASB over 80 mm cl4sp
11	240	7.3	3.7/3.7	32	130 mm l5sp
12	255	4.6	3.7/3.7	32	130 mm l5sp
13	250	6.1	3.7/3.7	32	130 mm l5sp

Note: PASB, permeable asphalt-stabilised base.
[a] The particle size distributions for these materials are provided in Table 13.

Table 12. Basic concrete properties of Mn/ROAD cells.

Cell	Modulus of rupture (28 day) (MPa)	Modulus of elasticity (28-day) (MPa)	Thermal coefficient (με/°C)	Permanent curl/ warp effective temperature difference (°C)
5	4.3	25,500	8.1	−0.1
6	3.9	31,500	8.1	0
7	4	27,000	8.1	0
8	3.5	31,000	8.4	0
9	3.9	29,500	9.8	0
10	4.3	21,500	8.1	0
11	5	26,000	6.7	0
12	4.6	28,500	8.8	0
13	4.7	27,500	8.8	0

Mn/ROAD is ideal in that accurate as-built construction, material characterisation and traffic data are available along with climate data from an on-site weather station. Extensive pavement performance data are also available throughout a 15-year time period. Another unique aspect about these test cells is that the built-in equivalent temperature difference between the top and bottom of the slab has been established for each test cell in a previous study (Vandenbossche 2003). Table 11 contains the basic design characteristics of the Mn/ROAD test cells. Table 12 shows the measured PCC properties and Table 13 provides the gradation specifications for the granular base and subbase layers as provided by the 1995 Minnesota Department of Transportation (Mn/DOT) Specification Standards. The inputs used in the MEDPG are based on the as-constructed data. The traffic data are based on the information collected using the weigh-in-motion at Mn/ROAD over the last 15 years and the climatic data used are from the Mn/ROAD weather station.

Table 13. Mn/DOT 1995 granular specifications (per cent passing).

	Base material			
Sieve size	cl3sp	cl4sp	cl5sp	PASB
38.1 mm	–	100	–	–
31.75 mm	–	–	–	100
25.4 mm	–	95–100	100	95–100
19.05 mm	–	90–100	90–100	85–98
12.7 mm	100	–	–	–
9.525 mm	95–100	80–95	70–85	50–80
No. 4	85–100	70–85	55–70	20–50
No. 10	65–90	55–70	35–55	0–20
No. 20	–	–	–	0–8
No. 40	30–50	15–30	15–30	0–5
No. 200	8–15	5–10	3–8	0–3

Notes: Special crushing requirements (sp): cl3sp and cl4sp, crushed/fractured particles are not allowed; cl5sp, 10–15% crushed/fractured particles are required; PASB, permeable asphalt-stabilised base.

The built-in temperature differences for the Mn/ROAD pavement cells are known to be equal to zero in all cases but in Cell 5, which has an built-in equivalent temperature difference of −0.1°C (very close to zero) (Vandenbossche 2003). The actual values of this parameter differ drastically from the assumed constant value of −5.5 °C that was assigned to all sites used in the cracking regression model implemented in the MEPDG.

A summary of the predicted and observed transverse cracking is provided in Table 14. Two separate runs of the MEDPG were performed for each cell. The first run was made using the actual measured built-in equivalent temperature difference. As shown in Table 14, the predictions of the MEPDG using the measured built-in equivalent temperature difference are extremely divergent from the actual observed performance. This can also be seen in Figure 18 for Cell 11 at Mn/ROAD. In an attempt to improve the performance prediction, a second run was made based on the MEPDG default built-in equivalent temperature difference of −5.5°C. As a result, a drastic improvement is seen in the prediction of the measured distress for all cells except Cells 5, 6 and 8. This indicates that it is most likely beneficial to use the default value of −5.5°C even if additional information is available for defining the actual built-in equivalent temperature difference. Previous work by Gutierrez (2008) supports this recommendation.

9. Summary and conclusions

The treatment of the permanent built-in temperature difference in the MEPDG deserves study because it was

Table 14. MEPDG cracking analysis of Mn/ROAD Cells 5–13.

Cell	5	6	7	8	9	10	11	12	13
Surveyed distress (%)	15	0	0	0	0	0	9	0	0
Predicted distress with known built-in temperature difference (%)	100	100	99	100	97	1	81	8	99
Predicted with built-in = −5.5°C (%)	85	100	52	94	54	0	2	0	42

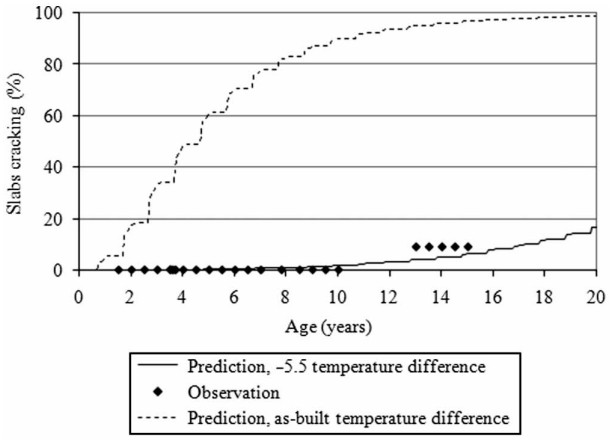

Figure 18. Observed vs. predicted cracking using default and measured built-in temperature differences for MnROAD Cell 11.

developed as a constant value during the calibration of the MEPDG performance models but is left as a modifiable input for users. The construction, curing and ageing of concrete pavements in different climates can be expected to result in the development of different effective temperature gradients in the slab due to both built-in factors as well as transient effects due to ambient environmental conditions during service. These different effective temperature gradients would produce different degrees of slab deformation (i.e. curling and warping) and the resulting slab stresses. Therefore, it is reasonable to expect that a reference pavement would perform differently under a given traffic stream in different climates. Considered differently, one would expect that analyses would show that different values of built-in effective temperature gradients would be required to offset the effects of transient gradients to produce constant levels of cracking at various test sites.

This study showed that there appears to be a single value of effective built-in temperature difference (-6.5°C) that minimises JPCP fatigue damage and transverse cracking predicted using the MEPDG for normally distributed traffic conditions, regardless of local environmental conditions. This value is very nearly equal to the MEPDG default input value of -5.5°C that was obtained through the nationwide model calibration process.

The effects of differences in ambient climatic conditions on the built-in gradient required to minimise cracking were more evident if all traffic loads were forced into a single hour each day with peak positive or negative temperature differences. The resulting temperature differences (built-in and transient) were not equal, however. In the case of negative (night-time) conditions, they were not even of opposite sign.

The effects of changes in the geometric design of the slab were also evaluated. Changing the thickness of the reference slab resulted in slight changes in the distribution of resulting transient gradients, but no significant changes in the built-in gradient required to minimise JPCP fatigue damage and cracking. Changing the slab length also did affect the built-in gradient required to minimise JPCP fatigue damage and cracking.

Based on this study, it appears that the most reasonable MEPDG performance prediction results for pavements with typical traffic patterns in most environments will be obtained by using the MEPDG-recommended default value for built-in temperature difference (-5.5°C). Other work has shown that predicted cracking agrees most closely with observed cracking levels if the default built-in equivalent temperature difference is used rather than a site-specific value. Further study is needed to develop a more rational way to incorporate site-specific local built-in equivalent temperature differences into MEPDG pavement designs.

Acknowledgements

The authors would like to extend their sincere gratitude to the Federal Highway Administration for providing some of the funding for this research effort.

Notes

1. Email: fem15@pitt.edu
2. Email: jjg39@pitt.edu
3. Email: jim.sherwood@dot.gov

References

ARA, Inc., ERES Division, 2004. *Guide for Mechanistic–Empirical Design of New and Rehabilitated Pavement Structure*. Final Report NCHRP 1-37A.

Barenberg, E.J., *et al.*, 2005. *Review Comments on the 2002 MEDG for New Concrete Pavements prepared for NCHRP 1-40A (02)*.

Beckemeyer, C., Khazanovich, L., and Yu, T., 2002. Determining amount of built-in curling in jointed plain concrete pavement: case study of Pennsylvania I-80. *Transportation Research Record: Journal of the Transportation Research Board*, 1809, 85–92.

Byrum, C., 2000. Analysis by high-speed profile of jointed concrete pavement slab curvatures. *Transportation Research Record: Journal of the Transportation Research Board*, 1730, 1–9.

Coree, B., 2005. *Implementing the Mechanistic–Empirical Pavement Design Guide: Technical Report*. Ames, IA: Iowa State University. Report prepared for the Iowa Highway Research Board (IHRB) Project TR-509.

Gutierrez, J.J., 2008. *Evaluating the JPCP Cracking Model of the Mechanistic–Empirical Pavement Design Guide*. Thesis (Degree Master of Science in Civil Engineering). University of Pittsburgh.

Gutierrez, J.J., 2008. *Evaluating the JPCP Cracking Model of the Mechanistic–Empirical Pavement Design Guide*. Thesis (Degree Master of Science in Civil Engineering). University of Pittsburgh.

Hall, K.D. and Beam, S., 2004. Estimating the sensitivity of design input variables for rigid pavement analysis with a Mechanistic–Empirical Design Guide. *Transportation Research Record: Journal of the Transportation Research Board*, l919, 65–73.

Kannekanti, V. and Harvey, J., 2005. *Sensitivity analysis of 2002 design guide rigid pavement distress prediction models*. Davis, CA: University of California. Report prepared for the California Department of Transportation.

Khazanovich, L. and Yu, T., 2005. Accounting for concrete shrinkage in the Mechanistic–Empirical Pavement Design Procedure. *In*: G. Pijaudier-Cabot, B. Gerard, and P. Acker eds. *Creep, shrinkage and durability of concrete structures*. London: Hermes Science Publishing, Ltd, 287–292.

Khazanovich, L., *et al.*, 2001. Development of rapid solutions for prediction of critical CRCP stresses. *Transportation Research Record: Journal of the Transportation Research Board*, 1778, 64–72.

Khazanovich, L., *et al.*, 2008. Adaptation of MEPDG for design of Minnesota low-volume Portland cement concrete pavements. *Transportation Research Record: Journal of the Transportation Research Board*, 2087, 57–67.

McCracken, J., Asbahan, R., and Vandenbossche, J.M., 2008. *Evaluating the cracking predicted by the MEPDG using results from the S.R.-22 smart pavement study.* Final Report for Pennsylvania Department of Transportation, Report No. PA-510601/WO-003.

National Oceanic and Atmospheric Administration, 2007. Available from: www.noaa.gov.

Rao, S. and Roesler, J.R., 2005. Characterizing effective built in curling from concrete pavement field measurements. *Journal of Transportation Engineering*, 131 (4), 320–327.

Vandenbossche, J.M., 2003. *Interpreting falling weight deflectometer results for curled and warped Portland cement concrete pavements*. Thesis (Degree Doctor of Philosophy in Civil Engineering). University of Minnesota.

Vandenbossche, J.M., *et al.*, 2009. Comparison of measured vs. predicted performance of jointed plain concrete pavements using the Mechanistic–Empirical Pavement Design Guide. *International Journal of Pavement Engineering*, under review.

Well, S.A., Phillips, B.M., and Vandenbossche, J.M., 2006. Quantifying built-in construction gradients and early-age slab shape to environmental loads for jointed plain concrete pavements. *International Journal for Pavement Engineers*, 7 (4), 275–289.

Well, S.A., Phillips, B.M., and Vandenbossche, J.M., 2006. Quantifying built-in construction gradients and early-age slab shape to environmental loads for jointed plain concrete pavements. *International Journal for Pavement Engineers*, 7 (4), 275–289.

Yu, T., *et al.*, 1998. Analysis of concrete pavement responses to temperature and wheel loads measured from instrumented slabs. *Transportation Research Record: Journal of the Transportation Research Board*, 1639, 94–101.